Vol. 377: 19–32, 2009
doi: 10.3354/meps07837

MARINE ECOLOGY PROGRESS SERIES
Mar Ecol Prog Ser

Published February 26

OPEN ACCESS

Contribution of N_2 fixation to new production in the western North Pacific Ocean along 155° E

Takuhei Shiozaki, Ken Furuya*, Taketoshi Kodama, Shigenobu Takeda

Department of Aquatic Bioscience, Graduate School of Agricultural and Life Sciences, The University of Tokyo, Yayoi, Bunkyo-ku 113-8657, Japan

ABSTRACT: Nitrogen (N_2) fixation and nitrate assimilation activities were examined simultaneously using a ^{15}N tracer in February and March 2007 along the 155° E meridian from the equator to 44° N in the western North Pacific Ocean. N_2 fixation was detected only to the south of 28° N, where the nitrate + nitrite (N+N) concentration was <30 nM in the upper mixed layer; the concentration ranged from 12.8 to 152 µmol N m^{-2} d^{-1}. High N_2 fixation rates were observed from 16° N to 24° N, where relatively high dust depositions and low concentrations (<100 nM) of soluble reactive phosphorus (SRP) were observed. The depth-integrated nitrate assimilation in the euphotic zone showed no significant latitudinal trend, varying between 184 and 349 µmol N m^{-2} d^{-1} in the area from the equator to 24° N, where the water column was stable. Toward the north of 28° N, nitrate assimilation was enhanced, while N_2 fixation became insignificant. The contribution of N_2 fixation to new production (= N_2 fixation + nitrate assimilation) ranged from 2 to 37 %, and the highest contribution was observed at 24° N at the center of the subtropical gyre, where the highest N_2 fixation occurred. From the equator to 24° N, the coefficient of variation of nitrate assimilation was 20 %, while that of N_2 fixation was 80 %, indicating that the latter is more responsible for the latitudinal variation in the contribution of N_2 fixation to new production.

KEY WORDS: New production · N_2 fixation · Nitrate assimilation · f-ratio · Western North Pacific Ocean

INTRODUCTION

Depending on the nitrogen source, primary production in the sea is divided into new and regenerated production (Dugdale & Goering 1967). The former depends on newly available nitrogen, and the latter on regenerated nitrogen. In the open ocean, nitrate has been thought to be a major nitrogen source for new production, and its upward flux to the euphotic zone depends on stratification of the water column. Although nitrogen (N_2) fixation is defined to be included in new production, new production is determined as nitrate assimilation in general practice, and N_2 fixation is often ignored even in subtropical and tropical oceans because its contribution to new production was thought to be negligible (McCarthy & Carpenter 1983). However, recent biogeochemical stoichiometric estimates and direct measurements of N_2 fixation have indicated that contrary to the previous assumption, N_2 fixation does contribute significantly to new production (Karl et al. 1997, Dore et al. 2002, Capone et al. 2005). Karl et al. (1997) and Dore et al. (2002) found that N_2 fixation contributed half of the new production at Stn ALOHA (22.75° N, 158° W). A similar estimate was reported by Capone et al. (2005), who concluded that N_2 fixation by *Trichodesmium* corresponds to half or more of the upward nitrate flux in the western subtropical and tropical North Atlantic Ocean.

However, despite the fact that the importance of N_2 fixation in new production has been shown by these studies, the exact contribution of N_2 fixation to new production on a global scale is still unknown. This is primarily because of our limited geographical and sea-

*Corresponding author. Email: furuya@fs.a.u-tokyo.ac.jp

sonal understanding of the N_2- and nitrate-based new production. Although recent model studies have shown there is large geographical variation in the magnitude of N_2 fixation (Deutsch et al. 2001, 2007, Lee et al. 2002, Moore et al. 2004), the western subtropical and tropical Pacific Ocean is one of the areas in which direct measurements of both N_2- and nitrate-based new production have not been carried out extensively.

The western subtropical and tropical areas of the North Pacific Ocean are characterized by the presence of warm water in the upper mixed layer, which results in stable stratification (Yan et al. 1992). Under such conditions, the upward flux of nitrates becomes suppressed. Therefore, the latitudinal distribution of nitrate assimilation is expected to be generally uniform. In addition, the western North Pacific Ocean is located near the Asian continent and receives episodic iron supply as a result of Asian dust. The iron requirement for diazotrophic growth is considerably higher than that for algal growth in the presence of fixed nitrogen, and the diazotrophic distribution depends on the iron supply (Falkowski 1997). Since the dust deposition flux in the North Pacific varies latitudinally (Jickells et al. 2005), the N_2 fixation activity and its contribution to new production are also expected to vary with latitude.

In the present study, the relative importance of N_2 fixation in new production along a north–south transect in the western subtropical and tropical Pacific Ocean is examined by directly determining the N_2 fixation and nitrate assimilation; in this manner, a possible latitudinal variation in the contribution of N_2 fixation to new production is also examined. Although recent studies address the significance of nitrification processes in the concept that the assimilation and/or upward flux of nitrate is balanced with the nitrate-based new production (Dore & Karl 1996, Yool et al. 2007, Raimbault & Garcia 2008), the assimilation and/or upward flux of nitrate is assumed to represent the nitrate-based new production in most studies (Capone et al. 2005, Kawakami & Honda 2007, Prakash et al. 2008). The present study is based on this latter assumption.

MATERIALS AND METHODS

Experiments were conducted on board RV 'Mirai' in the western tropical, subtropical, and subarctic Pacific Ocean along 155° E from 26 February to 23 March 2007. Routine casts were conducted for nutrients and chlorophyll *a* (chl *a*) at almost every degree along 155° E (open circles in Fig. 1). Hydrographic data were collected using a SeaBird SBE 911plus CTD system.

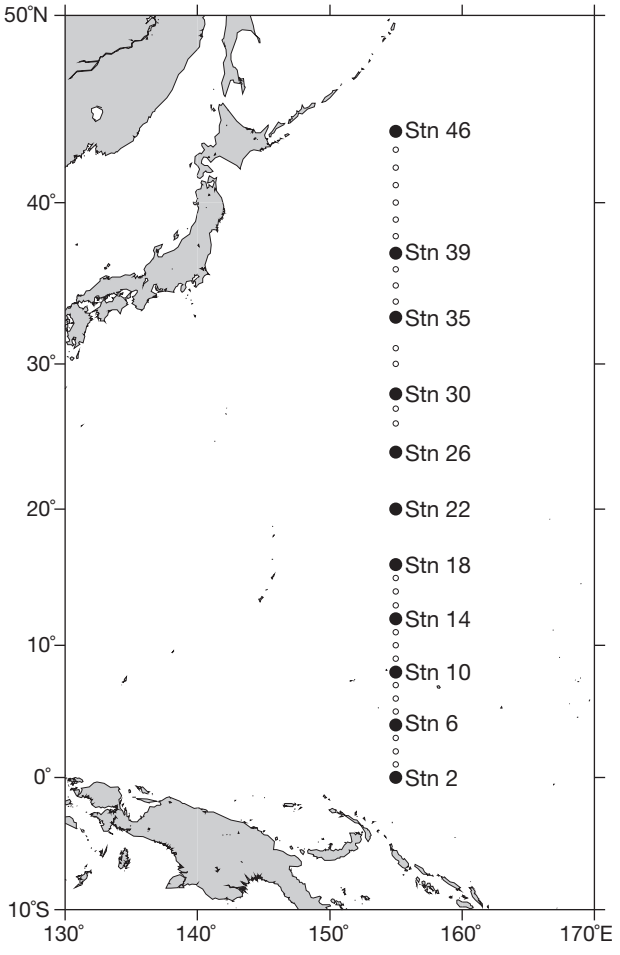

Fig. 1. Sampling stations in the western North Pacific Ocean during the MR07-01 cruise. ● and ○ indicate stations for ^{15}N and ^{13}C assimilation experiments, and those only for routine casts of CTD, respectively

Just before sampling, the depth profiles of light intensity were determined using a freefall SeaWiFS profiling multichannel radiometer system (Satlantic). The euphotic zone was defined as the upper water column down to the depth at which the downward photosynthetically active radiation (PAR) was 1% of the value just below the surface. Experiments to determine ^{15}N and ^{13}C assimilation experiments were conducted using additional casts conducted every 4° N (closed circles in Fig. 1), and these samples were collected in an acid-cleaned bucket and Niskin-X bottles (General Oceanics) from those layers having surface light intensities of 100, 50, 25, 10 and 1%. The samples used for the determination of nutrients and chl *a* were collected from layers within a depth of 0 to 200 m in the case of both routine and additional casts.

Mixed layer depth and Brunt-Väisälä frequencies. Brunt-Väisälä frequencies were calculated from the

vertical density profiles determined by the CTD using the equation given by Millard et al. (1990). The mixed layer depth (MLD) was defined as the depth at which sigma-t increased by 0.125 from the 10 m depth (Levitus 1982).

Nutrients, chl *a* and dust deposition flux. Immediately after sampling, the nutrient concentrations of nitrate, nitrite, soluble reactive phosphorus (SRP) and ammonium were determined by colorimetry using a TRAACS-800^{TM} (Bran+Luebbe) analyzer (Hansen & Koroleff 1999). When the nutrient concentrations were <0.1 µM, the concentrations of nitrate + nitrite (N+N) and SRP were analyzed using a supersensitive colorimetric system (detection limit, 3 nM) that consisted of an Auto Analyzer II (Technicon) connected to a liquid waveguide capillary cell (LWCC, World Precision Instruments). Detailed information on the blank N+N and SRP and the detection limits are described elsewhere (Hashihama et al. in press). Since a preliminary examination showed that nitrites were barely detectable in N+N depleted water, the N+N concentrations measured here can be considered to correspond purely to the nitrate concentration; the measured concentrations were used in nitrate assimilation experiments. The concentrations of N+N and SRP at the surface water were also measured semi-continuously by using the supersensitive colorimetric system from the equator to 30° N (T. Kodama unpubl.), and these were used as an indicator of the oligotrophic ocean.

Seawater samples (0.5 l) were filtered onto 25 mm Whatman GF/F filters for fluorometric determination of chl *a* concentrations using a Turner Design 10-AU fluorometer after extraction with N,N-dimethylformamide (Suzuki & Ishimaru 1990).

Atmospheric dust deposition was simulated by the spectral radiation-transport model for aerosol species (SPRINTARS; Takemura et al. 2000). The fluxes at each location were averaged for 2 wk prior to our study period (Hashihama et al. in press).

Nitrate assimilation experiments. Nitrate assimilation experiments were conducted using the Michaelis-Menten kinetics approach to correct the overestimation caused by the excessive use of ^{15}N tracer (Harrison et al. 1996, Kanda et al. 2003) in the N+N depleted (<0.1 µM) region (from the equator to 28° N). The samples were poured into 3 acid-cleaned 2 l polycarbonate bottles, and then ^{15}N-labeled nitrate was added to each bottle (99.8 atom% ^{15}N; Shoko) to adjust the final tracer concentrations to 10, 100 or 2000 nM. At the stations where the ambient N+N concentrations at the surface were more than 1 µM, ^{15}N-labeled nitrate was added to the samples to adjust the final tracer concentration to 10 nM. The samples collected (4.5 l) for estimating the natural ^{15}N abundance of particulate organic nitrogen (PON) were filtered immediately at the beginning of the incubation. The samples for incubation were wrapped in neutral-density screens to adjust each light level and then placed in an on-deck incubator cooled by flowing surface seawater. The incubation was terminated within 4 h by gentle vacuum filtration (<200 mm Hg) of the seawater samples through a precombusted GF/F filter. The filters were kept frozen (–20°C) until on-shore analyses were performed. In the shore laboratory, the filters were dried at 50°C overnight, exposed to HCl fumes for 2 h, and then dried again. The concentrations of particulate organic nitrogen and carbon were determined using a Flash EA elemental analyzer (Thermo Electron). Isotopic analysis was conducted using a DELTA^{plus} XP mass spectrometer (Thermo Electron) that was connected to the elemental analyzer.

The nitrate assimilation rates (ρ) were calculated using Eq. (1), which was proposed by Kanda et al. (1985):

$$\rho = \frac{P_f}{t} \times \frac{I_f - I_0}{I_S - I_0} \quad (1)$$

where P_f is the final concentration of particulate organic nitrogen, t is the incubation time, I_f is the atom% of ^{15}N in particulate nitrogen after incubation, I_0 is the atom% of ^{15}N in particulate nitrogen at the beginning of the incubation and I_S is the atom% of ^{15}N in the substrate after the addition of the tracer.

At the stations where the kinetics experiments were conducted, we used the Michaelis-Menten equation (Eq. 2) to calculate the *in situ* nitrate assimilation rates (ρ_k):

$$\rho_k = \frac{\rho_{max} \times S}{K_S + S} \quad (2)$$

Here ρ_{max} is the maximum assimilation rate, K_S is a half-saturation constant and S is the ambient nitrate concentration. However, since the parameters ρ_{max} and K_S are unknown, the concentration-dependent nitrate assimilation rates (ρ_n) calculated by Eq. (1) were fitted to Eq. (3):

$$\rho_n = \frac{\rho_{max} \times (S + S_n)}{K_S + (S + S_n)} \quad (3)$$

where S_n is the concentration of each tracer (10, 100 and 2000 nM). Then, ρ_{max} and K_S were estimated using the quasi-Newton method. Finally, ρ_k was calculated from Eq. (2) using the estimated values of ρ_{max} and K_S. The daily assimilation rates were approximately estimated by multiplying the hourly rates by 16, the value 16 being derived from the relationship between daytime and nighttime assimilation rates obtained from observations for 2 yr in the Bermuda Atlantic Time Series Study (BATS) in the subtropical North Atlantic Ocean (Lipschultz 2001).

Kinetics experiments were conducted at stations that were N+N depleted, i.e. Stns 2 to 30. Since S exceeded 1 µM at a light depth of 1% at Stns 2, 6 and 10, the ρ_k values were calculated using the S values of those samples to which 100 nM of the tracer was added. A K_S value that was estimated to be negative was not used in the calculation of ρ_k (1 out of 37 determinations). The coefficient of determination of the quasi-Newton method ranged from 0.51 to 1.00 with a mean of 0.91. Since S values at Stns 39 and 46 were much higher than the added amounts of the tracer, varying above 4.8 µM, it was deduced that ^{15}N tracer was highly diluted in incubation bottles and its assimilated amount was too low to be detected.

N_2 fixation and primary production experiments. The rates of N_2 fixation and primary production were measured by a dual isotopic technique (using $^{15}N_2$ and ^{13}C). Two identical samples were collected in acid-cleaned 4.5 l polycarbonate bottles. ^{13}C-labeled sodium bicarbonate (99 atom% ^{13}C; Cambridge Isotope Laboratories) was added to each bottle to achieve a final tracer concentration of 200 µM before sealing it with a thermoplastic elastomer cap. Then, using a gas-tight syringe, 2 ml of $^{15}N_2$ gas (99.8 atom% ^{15}N; Shoko) was added to each bottle. The initial concentration of dissolved N_2 was calculated by using the equation given by Weiss (1970). After these treatments, neutral-density screens were employed to adjust each light level. The samples were incubated in an on-deck incubator, and the incubation was terminated after 24 h. The samples used for experiments to determine the natural ^{15}N abundance of PON are identical to the ones used in the nitrate assimilation experiments. The conditions for the pretreatment and actual analysis were also maintained identical to those in the nitrate assimilation experiments. The rates of N_2 fixation and primary production were calculated using the equations proposed by Montoya et al. (1996) and Hama et al. (1983), respectively.

***f*-ratio.** The f-ratio is defined as the ratio of new production to the total production (Eppley & Peterson 1979). Conventionally, it is calculated using the assimilation of new and regenerated nitrogen or using carbon assimilation, under the assumption that the total production calculated on the basis of carbon can be converted to the total production on the basis of nitrogen using the Redfield ratio of 6.6 (Eq. 4, where ρ is the assimilation rate) (Falkowski et al. 2003). Since N_2 fixation is generally considered to be negligible, it is not considered in this equation (McCarthy & Carpenter 1983). However, since it has been proved that N_2 fixation does significantly contribute to new production in oligotrophic oceans (e.g. Karl et al. 1997, Capone et al. 2005), we corrected Eq. (4) by adding the magnitude of N_2 fixation to the new production and calculated f_{+N_2} using Eq. (5).

$$f = \frac{\text{new production}}{\text{new + regenerated production}}$$

$$\cong \frac{\rho NO_3^-}{\rho NO_3^- + \rho NH_4^+ + \rho NO_2^- + \rho DON}$$

$$\cong \frac{\rho NO_3^- \times 6.6}{\rho CO_2} \quad (4)$$

$$f_{+N_2} = \frac{(\rho NO_3^- + \rho N_2) \times 6.6}{\rho CO_2} \quad (5)$$

Note that we have ignored the contribution of nitrification in Eq. (5), even though it has been pointed out by Fernández et al. (2005) that the effect of nitrification on the estimation of the f-ratio is not actually negligible.

RESULTS

Hydrography and water column stratification

The western Pacific Ocean warm pool, which has a sea surface temperature (SST) of >29°C (Yan et al. 1992), extends from the equator to 5° N (Fig. 2a). The western Pacific subtropical gyre was distributed between a salinity front at 15° N and a distinct thermal front associated with Kuroshio (Fig. 2a,b). The surface salinity was highest at 24° N, which is the center of the subtropical gyre (Tomczak & Godfrey 1994). A transition area between the warm pool and the subtropical gyre, where a remarkable thermal dome was observed, is referred to as the frontal zone in the present study (Fig. 2b). The north equatorial current flows in this frontal zone (Tomczak & Godfrey 1994). The largest horizontal temperature gradient in the upper ocean was observed to the north of 34° N, corresponding to the Kuroshio Extension. The subarctic boundary, which is characterized by a vertical isohaline of 34 and cold waters (<4°C) in the upper mixed layer, was located to the north of the Kuroshio Extension (Favorite et al. 1976).

The MLD from the equator to 28° N roughly corresponded to the depth where the Brunt-Väisälä frequencies were >0.005 s^{-1} and tended to deepen northward (filled triangles in Fig. 3). The MLD was less than 200 m from 30° N to 33° N and from 41° N to 42° N. The water column was well stratified from the equator to 24° N, and it was relatively unstable at 28° N (Fig. 3). To the north of 30° N, the water column was well mixed.

Nutrients, chl *a* and dust deposition flux

The N+N concentration showed a 2-layer distribution from the equator to the northern part of the sub-

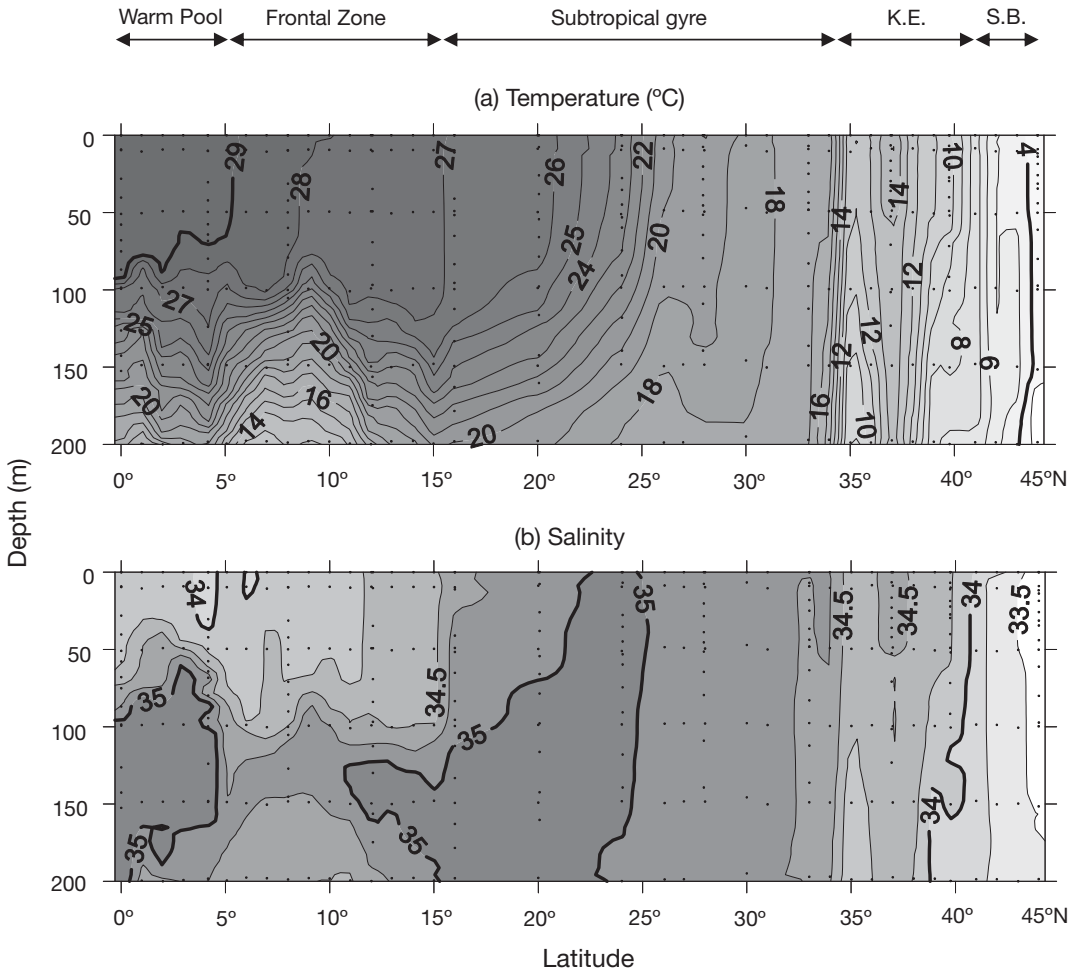

Fig. 2. Vertical profiles of (a) temperature (°C) and (b) salinity along 155° E. Isotherms of 4°C and 29°C, and isohalines of 34 and 35 are highlighted (i.e. thicker lines) in (a) and (b), respectively. Dots indicate depths of water sampling. K.E. and S.B. denote Kuroshio Extension and subarctic boundary, respectively

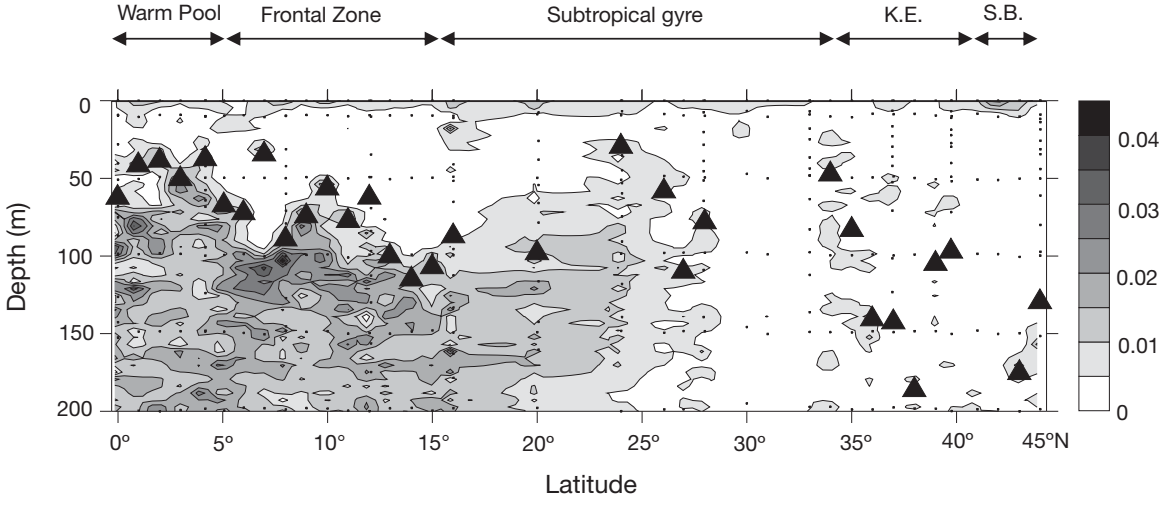

Fig. 3. Vertical profiles of Brunt-Väisälä frequency (s^{-1}) along 155° E. (▲) Bottom of the mixed layer depth

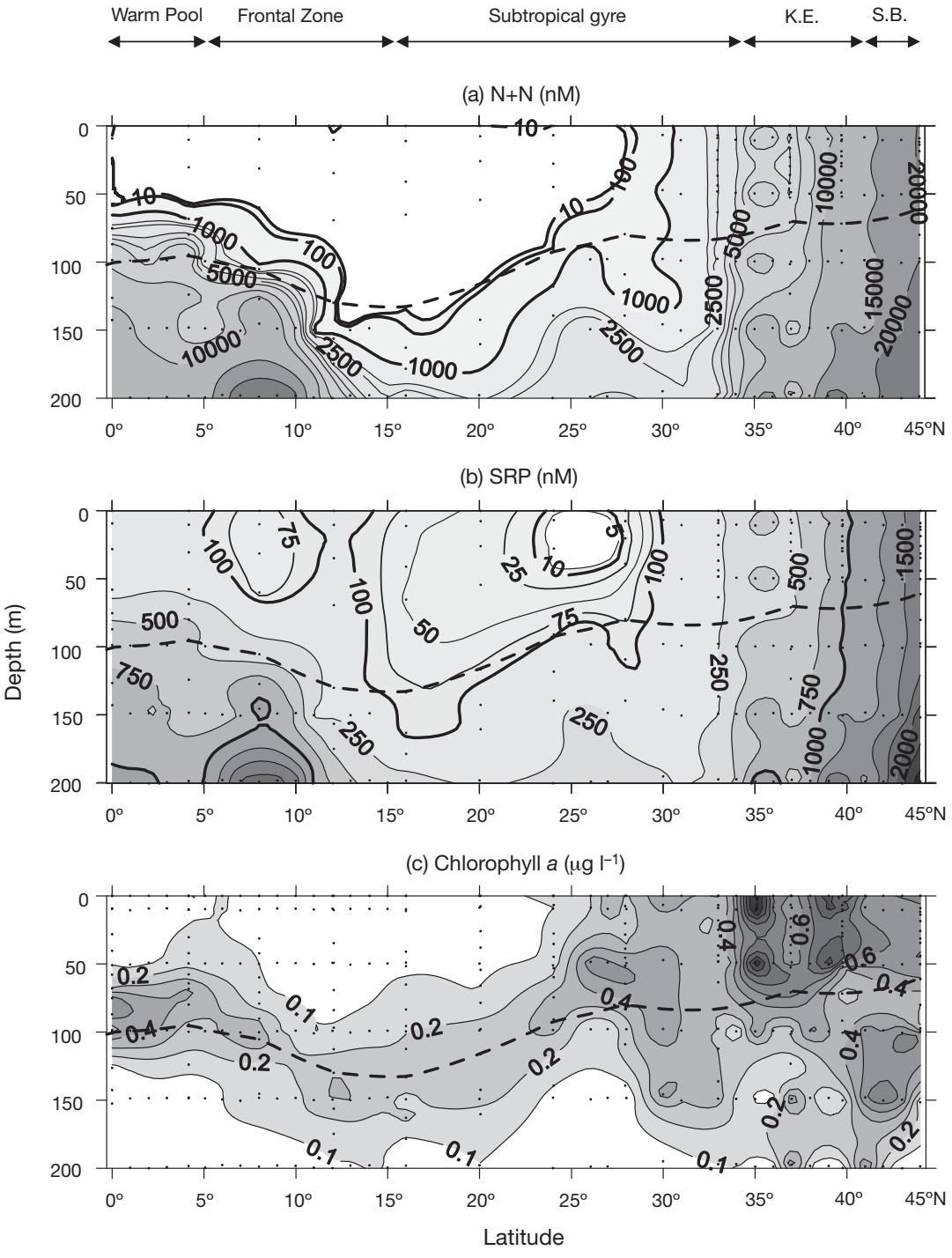

Fig. 4. Vertical profiles of (a) N+N (nM), (b) SRP (nM) and (c) chl *a* (μg l^{-1}) along 155° E. Isopleths of 10, 100 and 1000 nM N+N and those of soluble reactive phosphorus (SRP) are highlighted (i.e. thicker lines) in (a) and (b), respectively. Dashed lines indicate the 1% light depth

tropical gyre, with a nitracline present at subsurface depths (Fig. 4a). In the Kuroshio Extension and subarctic boundary, N+N was uniformly distributed in the upper 200 m of the water column in which N+N concentrations increased northward. The N+N depleted waters (concentration of 8 to 27 nM) at the surface extended from the equator to 28° N (Table 1); this is defined as the N+N depleted region in this study. The N+N concentration above the nitracline at the equator was higher than that in the northern region.

Table 1. Depth-integrated NO_3^- assimilation (ρNO_3^-) (µmol N m^{-2} d^{-1}), N_2 fixation (ρN_2) (µmol N m^{-2} d^{-1}) and primary production (ρCO_2) (mmol C m^{-2} d^{-1}) with environmental parameters (temperature [°C], salinity, chl *a* [µg l^{-1}], N+N [nM] and SRP [nM]) and abundance of *Trichodesmium* (filaments l^{-1}) at the surface. nd = not detectable (below analytical limit of detection), na = no data available

Station	Latitude (°N)	Temp. (°C)	Salinity	Chl *a* (µg l^{-1})	N+N (nM)	SRP (nM)	*Trichodesmium* (filaments l^{-1})	ρNO_3 (µmol N m^{-2} d^{-1})	ρN_2 (µmol N m^{-2} d^{-1})	ρCO_2 (mmol C m^{-2} d^{-1})
2	0	29.9	34.1	0.07	24	188	2	330	42.5	23.1
6	4	29.4	33.9	0.11	12	143	0	184	38.2	16.8
10	8	28.4	34.2	0.08	10	59	3	252	12.8	25.4
14	12	27.8	34.3	0.04	15	118	1	325	45.8	18.8
18	16	27.1	34.7	0.06	8	71	5	349	91.8	18.2
22	20	26.6	34.9	0.09	8	45	4	250	31.5	18.5
26	24	23.8	35.0	0.10	8	6	0	258	152	22.8
30	28	19.9	34.9	0.29	27	17	4	1050	25.4	31.6
35	33	18.8	34.8	0.31	2220	228	0	1170	nd	35.6
39	37	14.8	34.6	0.59	4810	444	0	na	nd	35.4
46	44	3.2	33.2	0.65	20300	1690	0	na	nd	40.6

The SRP concentrations at the surface ranged from 6 to 188 nM in the N+N depleted region (Fig. 4b & Table 1), and according to the Redfield ratio, SRP was generally more abundant than N+N above the nitracline. Nonetheless, surface waters with lower SRP concentrations than neighboring waters were located at 8° N and from 16° N to 28° N. In particular, the SRP concentration near the center of the subtropical gyre was as low as 4 nM. To the north of 30° N, the SRP distribution was generally similar to the N+N distribution; in other words, SRP was vertically uniform and increased toward the north, reaching a maximum of 1.7 µM at 44° N. The NH_4^+ concentration was consistently low (<0.1 µM) throughout the water column to the south of 41° N, while it tended to increase to 0.2 µM to the north of 41° N (data not shown).

The subsurface chl *a* maximum (SCM) developed in the N+N depleted region, and it generally corresponded to a light depth of 1%. (Fig. 4c). In the warm pool, the SCM was observed above the thermocline at depths of around 80 m; here, the chl *a* concentrations (~0.4 µg l^{-1}) were relatively higher than those in the northern region. The SCM deepened from 6° N to 10° N, along with a deepening of the nitracline. The SCM gradually became shallower from 10° N to 28° N along with an upsloping of the nitracline, and the chl *a* concentrations increased to 0.4 µg l^{-1} at 28° N. To the north of 28° N, there was no SCM, and the vertical profiles of chl *a* were almost uniform above the light depth of 1%.

During our study period, the dust deposition flux simulated by SPRINTARS was assessed to be relatively low in the warm pool and frontal zone, while it icreased toward the north of the subtropical gyre (Fig. 5).

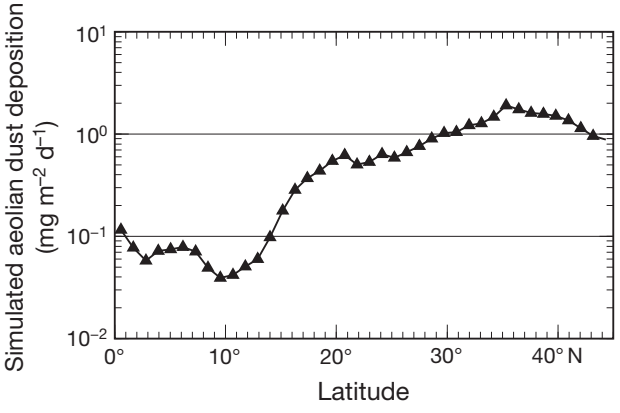

Fig. 5. Latitudinal distribution of atmospheric dust deposition as simulated by the SPRINTARS

Nitrate assimilation rate

The nitrate assimilation rate tended to be higher in the northern stations (Fig. 6a). In the area between the equator and 24° N, latitudinal tendency was not observed in the nitrate assimilation, which ranged from 0.13 to 4.55 nmol N l^{-1} d^{-1} in the euphotic zone. The nitrate assimilation showed vertical maxima with depths occurring at the surface and around the bottom of the euphotic zone in the warm pool, between 25 and 10% light depths in the frontal zone and the southern and center of the subtropical gyre, and at the surface in the northern part of the subtropical gyre. The nitrate assimilation positively correlated with the concentrations of N+N and chl *a* and the primary production, while it negatively correlated with the temperature in the upper mixed layer (Table 2).

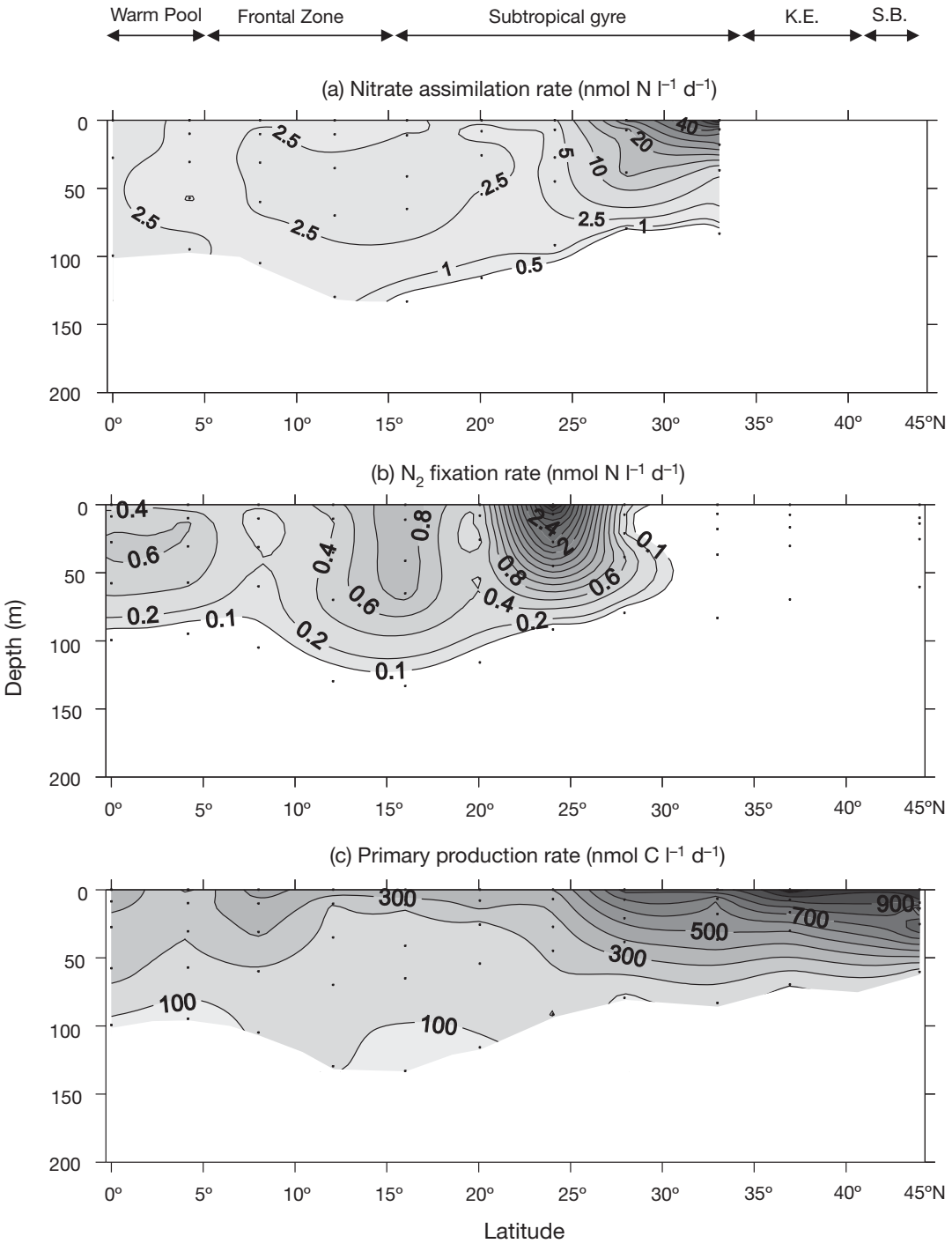

Fig. 6. Vertical profiles of (a) nitrate assimilation rate (nmol N l^{-1} d^{-1}), (b) N_2 fixation rate (nmol N l^{-1} d^{-1}) and (c) primary production (nmol C l^{-1} d^{-1}) along 155° E

N_2 fixation rate

N_2 fixation activity was detected in the N+N depleted region (Fig. 6b). The highest N_2 fixation rate observed at the surface of 24° N in the center of the subtropical gyre was 1 order of magnitude higher than that observed at the other stations. The N_2 fixation activity at 8° N was extremely low when compared with that in the neighboring areas. A vertical maximum of the N_2 fixation rate was observed at the surface except in the case of the warm pool where the maximum N_2 fixation rates occurred at light depths of

Table 2. Pearson's correlation matrix among water properties in the upper MLD from the equator to 33° N (n = 30). $^{*}p < 0.05$, $^{**}p < 0.001$

	Temperature	Salinity	N+N	SRP	Chl *a*	ρCO_2	ρN_2	ρNO_3^-
Temperature	1							
Salinity	−0.64	1						
N+N	−0.79	0.25	1					
SRP	−0.28	−0.35	0.74	1				
Chl *a*	−0.93	0.40	0.77	0.38	1			
ρCO_2	−0.59	0.29	0.42	0.15	0.62	1		
ρN_2	0.10	0.35	−0.33	−0.47*	−0.29	−0.13	1	
ρNO_3^-	−0.66**	0.31	0.60**	0.35	0.70**	0.82**	−0.24	1

25 and 50%. The maximum N_2 fixation rates ranged between 0.24 and 3.62 nmol N l^{-1} d^{-1}. No N_2 fixation activity was detected at the 1% light depth at any of the stations. The *Trichodesmium* concentration at the surface was very low, a few filaments per liter at the most (Table 1), and the heterocystous endosymbiont *Richelia* at the surface was found only at 20° N with 2 heterocysts per liter in the present study (S. Kitajima pers. comm.). Therefore, the N_2 fixation in this study can probably be ascribed to pico- and nanoplanktonic diazotrophs. N_2 fixation has no significant correlation with nitrate assimilation and primary production in the upper mixed layer, which indicates that the factors controlling N_2 fixation are different from the above-mentioned 2 parameters. This was probably because contribution of N_2 fixation to primary production from the equator to 33° N was much lower (0 to 4.39%) than of nitrate assimilation (6.53 to 21.7%) (Table 1). Thus, the regional variability in N_2 fixation was unlikely reflected in that of primary production, and in chl *a* compared with that of nitrate assimilation. In contrast, N_2 fixation negatively correlated with SRP (Table 2).

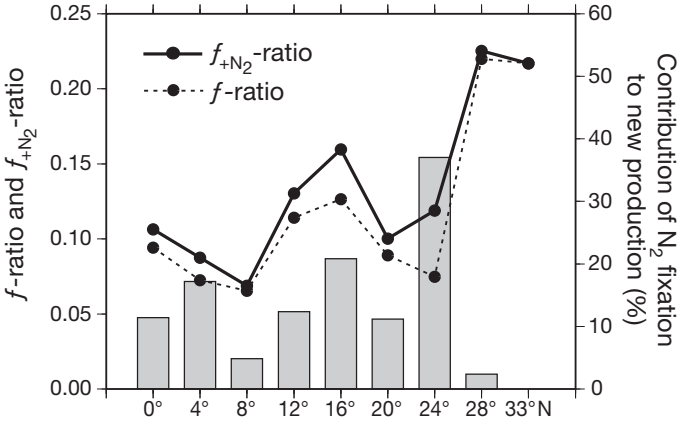

Fig. 7. Latitudinal distribution of depth-averaged f-ratio, f_{+N_2}-ratio and the contribution of N_2 fixation to new production (%) in the euphotic zone along 155° E

Primary production

The depth-integrated primary production remained constant toward the south of 24° N, while it increased toward the north of 24° N (Fig. 6c). This latitudinal trend was similar to that observed in the case of nitrate assimilation. The primary production showed a vertical maximum to the south of 24° N, varying from 312 to 455 nmol C l^{-1} d^{-1}. The maximum primary production occurred at the surface at 9 stations, but at 50% light depth at 2 other stations located at 4 and 18° N.

f-ratio and contribution of N_2 fixation to new production

The distributions of the depth-averaged f- and f_{+N_2}-ratios in the euphotic zone are shown in Fig. 7. The f-ratio was less than 0.15 from the equator to 24° N, and it exceeded 0.2 to the north of 28° N. The mean f_{+N_2}-ratio from the equator to 28° N was 0.12, and this was significantly higher than the mean f-ratio of 0.10 ($p < 0.01$). Thus, although N_2 fixation contributed significantly to new production, its magnitude was, on average, small. The greatest difference between the f- and f_{+N_2}-ratios (0.04) was observed at 24° N in the center part of the subtropical gyre, where the N_2 fixation rates were the highest.

If we assumed that nitrate assimilation is regarded as the nitrate-based new production, the contribution of N_2 fixation to new production can be expressed as $100 \times N_2$ fixation rate/(N_2 fixation rate + nitrate assimilation rate) (Fig. 8). In our study, the contribution corresponded well with the distribution of N_2 fixation because nitrate assimilation showed insignificant latitudinal trends, except at 28° N. In the warm pool, the contribution of N_2 fixation tended to be high at subsurface layers. The highest depth-averaged contribution (37%) was observed at 24° N in the center of the subtropical region.

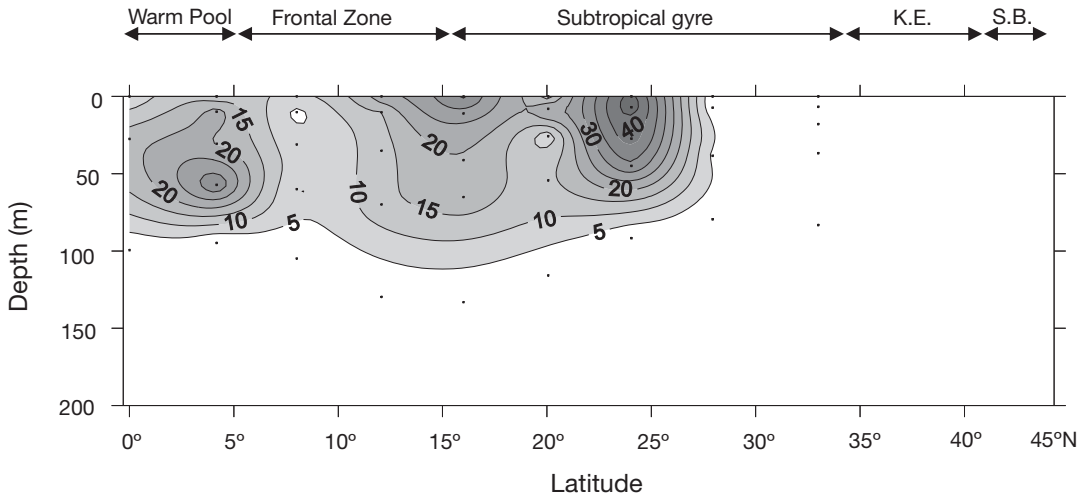

Fig. 8. Vertical profiles of the contribution of N_2 fixation to new production (%) along 155° E

DISCUSSION

Aufdenkampe et al. (2002) conducted nitrate and carbon assimilation experiments down to 0.1% light depth in the equatorial Pacific Ocean. They reported that the assimilation rates of both nitrate and C have a vertical maximum above 50 m throughout their study area, and that nitrate and C assimilation rates integrated from the surface to the 0.1% light depth have variations over a range 1.04 to 1.22 times (mean ± SD, 1.11 ± 0.03) and 1.10 to 1.42 times (1.19 ± 0.04) higher than those to the 1.0% light depth, respectively. Our observations that the vertical maxima of both nitrate and C assimilation occurred above the 10% light depths substantially support the results of Aufdenkampe et al. (2002). One exception was noted in the case of nitrate assimilation at the equator, where the assimilation rate was highest at the 1% light depth. Thus, while our integrated nitrate and C assimilation rates can be underestimated due to the lack of estimates below the 1% depths, a major portion of nitrate and C assimilation was detected in the water column. Regarding N_2 fixation, no activity was found at the 1% light depth in our study area, supporting the finding of Dore et al. (2002). Thus, we believe our incubation made in the upper 1% light level was suitable to obtain the integrated N_2 fixation.

Aufdenkampe et al. (2002) also conducted onboard *in situ* intercalibration experiments of nitrate assimilation in their study area. They reported that *in situ* nitrate assimilation rates integrated to the 1% light depth range from 1.13 to 1.79 times (mean ± SD, 1.37 ± 0.09) higher than those obtained by the onboard incubation. The differences in estimates between *in situ* and onboard incubations are probably a result of, at least partially, inadequate simulations of light and temperature conditions during the onboard incubation. While use of neutral density filters is a routine practice, the filters cannot create light conditions in the lower part of the euphotic zone. Furthermore, in our study there was a temperature difference of up to 5°C between the surface samples and the deepest samples. The difference probably caused a certain degree of underestimation in our estimate, because nitrate assimilation is sensitive to temperature (Harrison et al. 1996).

Nitrate assimilation rate in the western tropical and subtropical North Pacific Ocean

The present study is the first to present a latitudinal distribution of nitrate assimilation in the western tropical and subtropical North Pacific Ocean. Turk et al. (2001) reported nitrate assimilation rates under non-El Niño, moderate El Niño and strong El Niño conditions in the warm pool, where the magnitude of the nitrate assimilation rate was similar under the non-El Niño (150 ± 50 µmol N m^{-2} d^{-1}) and moderate El Niño (190 ± 100 µmol N m^{-2} d^{-1}) conditions, but was considerably higher under strong El Niño conditions (1160 ± 470 µmol N m^{-2} d^{-1}). During our cruise, the oceanic El Niño indices were 0.4 (February) and 0.1 (March) (NOAA National Weather Service www.cpc.ncep.noaa.gov/products/analysis_monitoring/ensostuff/ensoyears.shtml, accessed 14 July 2008), indicating a non-El Niño condition. The mean nitrate assimilation in the warm pool (257 µmol N m^{-2} d^{-1}) was comparable with that reported by Turk et al. (2001). In the subtropical gyre, the nitrate assimilation rates ranged between 250 and 1170 µmol N m^{-2} d^{-1} (Table1), and these were consistent with the results reported in previous stud-

ies on the subtropical Pacific Ocean (Table 3 in Kanda 2008).

The area of low nitrate assimilation from the equator to 24° N corresponded to stable stratified water (Figs. 3 & 6a), suggesting that the upward flux of nitrates was strictly limited by the strong stratification. In contrast, the water column to the north of 28° N was relatively unstable, and nitrate assimilation was elevated along with a relatively high nitrate supply. Thus, nitrate assimilation was largely controlled by upward fluxes of nitrates. Hence, on this basis, we can conclude that nitrate assimilation depends on the physical structure of the water mass. The present study, together with previous studies, shows that the nitrate assimilation rate is generally constant horizontally in the western tropical and subtropical North Pacific Ocean in the absence of the El Niño Southern Oscillation (ENSO) event and sporadic disturbance, including wind-induced mixing (Eppley & Renger 1988) and mesoscale eddy (McGillicuddy et al. 1998).

N_2 fixation in the western North Pacific Ocean

To the north of 16° N, the N_2 fixation activity at the surface was high, and the highest activity was observed in the center of the subtropical gyre (Fig. 6b). This area with high N_2 fixation had a higher dust deposition flux than did the southern regions (Fig. 5). Diazotrophs are known to require a considerably larger amount of iron for their growth than do other phytoplankton (Kustka et al. 2003). Hence, this suggests that iron supply from the atmospheric dust deposition probably influences the N_2 fixation activity in the western North Pacific Ocean. Furthermore, this area had relatively low SRP at the surface, thereby suggesting that phosphorus consumption may have been enhanced by the N_2 fixation (Hashihama et al. in press).

Owing to the high iron input, N_2 fixation is expected to be higher in the western North Pacific Ocean located near the Asian dust source than in the eastern area (Falkowski 1997, Jickells et al. 2005). However, the mean depth-integrated N_2 fixation (60.1 µmol N m^{-2} d^{-1}) in the subtropical gyre was similar to that reported at Stn ALOHA (Dore et al. 2002, Montoya et al. 2004, Grabowski et al. 2008), and is considerably lower than that reported in the eastern North Pacific Ocean (Montoya et al. 2004) (Table 3). While the abundance of *Trichodesmium* is known to be low in the western subtropical North Pacific Ocean (Asaoka & Marumo 1987), microplanktonic diazotrophic blooms were frequently reported in the eastern ocean by satellite and shipboard observations (Dore et al. 2008 and references, therein). By performing stoichiometric analysis, Dore et al. (2008)

Table 3. Comparison of published N_2 fixation rates using the $^{15}N_2$ method in the Pacific Ocean

Region	Dates	N_2 fixation (µmol N m^{-2} d^{-1})	Reference
North Pacific			
Western North Pacific			
Warm pool (0–5° N, 155° E)	Feb–Mar 2007	40.4	This study
Frontal zone (5–15° N, 155° E)	Feb–Mar 2007	29.3	This study
Subtropical gyre (15–34° N, 155° E)	Feb–Mar 2007	60.1	This study
Central part of subtropical gyre (24° N, 155° E)	Feb–Mar 2007	152	This study
Eastern North Pacific			
Stn ALOHA (22.75° N, 158° W)	Jul 2000–Jun 2001	40 (Nov)–115 (Jul)[a]	Dore et al. (2002)
	2000–2001	66[b]	Montoya et al. (2004)
	Apr 2004–Mar 2005	20.2 (Nov)–109 (Mar)	Grabowski et al. (2008)
Eastern North Pacific gyre (30° N[c], 125–160° W)	Jun–Jul 2002	520[b]	Montoya et al. (2004)
Eastern temperate oligotrophic region (34° N, 129° W)	Oct 2001	15	Needoba et al. (2007)
South Pacific			
Southwest Pacific near New Caledonia (21° S, 167° E)	Apr 2002–Oct 2005	151 (Apr)–703 (Feb)	Garcia et al. (2007)
Central and eastern South Pacific			
Marquesas archipelago (8° S[c], 141–134° W)	Oct–Nov 2004	110	Raimbault & Garcia (2008)
High nutrient low chlorophyll area (9° S[c], 133–123° W)	Oct–Nov 2004	70	Raimbault & Garcia (2008)
South Pacific gyre (26° S[c], 123–101° W)	Oct–Nov 2004	60	Raimbault & Garcia (2008)
Eastern border of the gyre (32° S[c], 100–81° W)	Oct–Nov 2004	30	Raimbault & Garcia (2008)
Chilean upwelling (34° S[c], 80–72° W)	Oc.–Nov 2004	90	Raimbault & Garcia (2008)

[a]Approximate values read from their Fig. 4B
[b]<10 µm fraction
[c]Central location of transects

suggested that at Stn ALOHA, the iron concentration is sufficiently high compared with the phosphate concentration, and a phosphate concentration of 6 to 89 nM in the upper 60 m is required for diazotrophic blooms. In the present study, the SRP was less than 6 nM in the center of the subtropical gyre, but it was very high in the other regions. Hence, N_2 fixation, except in the center of the subtropical gyre, was not affected by the presence of phosphate during our cruise. Since dust deposition is episodic, iron concentration near the Hawaiian Islands is known to be occasionally higher than that in the western North Pacific Ocean owing to fluvial and atmospheric inputs (Brown et al. 2005). Therefore, this episodic iron input can induce diazotrophic blooms. In the western North Pacific Ocean, in the absence of the island effect, the dominant source of iron in the surface is atmospheric dust (Jickells et al. 2005). Asian dust is known to show seasonal and areal variations (e.g. Tsunogai et al. 1985). Therefore, depending on the atmospheric dust inputs, the N_2-based new production in the western North Pacific Ocean probably varies with time and space.

Contribution of N_2 fixation to new production

The mean contribution of N_2 fixation to new production reported in the subtropical gyre (18%) was lower than that reported at Stn ALOHA (32 to 69%) by Karl et al. (1997) and Dore et al. (2002); however, the mean N_2 fixation rates were similar in both the cases (Dore et al. 2002, Montoya et al. 2004). Even the highest observed contribution of 37% at 24° N had a lower range of reported values. Dore et al. (2002) compared the N_2 fixation rates determined by $^{15}N_2$ incubation experiments with the sediment trap-derived values estimated from the nitrogen isotope composition of sinking particles, and found that the rates could account for only 18 to 55% (mean of 30%) of the trap-derived N_2 fixation rates. They ascribed this difference to the undersampling of microplanktonic diazotrophs by bottle incubations. Bottle incubations can only provide a more instantaneous perspective of the marine ecosystem than sediment-trap experiments, and thus, they may not reveal many details of the episodic bloom phenomena of microplanktonic diazotrophs. However, in the present study, we assumed that microplanktonic diazotrophs had only a minor effect on the N_2 fixation rates because we observed very few microplanktonic diazotrophs and performed our comparisons approximately on the same time scale.

Although we assume that nitrate assimilation is equal to nitrate-based new production, it must be noted that the former is influenced by nitrification (Dore & Karl 1996, Yool et al. 2007, Raimbault & Garcia 2008). Dore & Karl (1996) and Raimbault & Garcia (2008) reported that the nitrification rate ranges between 47 and 147% (Stn ALOHA), and 80 and 100% of the nitrate assimilation rate (the oligotrophic South Pacific gyre), respectively. Yool et al. (2007) synthesized previously published nitrification rates in the euphotic zone and constructed a global biogeochemical model. They estimated that approximately half the amount of nitrate consumed by phytoplankton is generated by nitrification on a global scale, and that the contribution of nitrification to nitrate assimilation is more than 70% in the oligotrophic ocean. Therefore, the contribution of N_2 fixation to new production in the present study is probably a conservative estimate, because in the presence of nitrification, a portion of the assimilated nitrate represents regenerated production. In contrast, our estimates of the f_{+N_2}-ratio were lower than those shown in Fig. 7, if we assume that a part of nitrate was produced by nitrification.

CONCLUSIONS

The present study has demonstrated that the contribution of N_2 fixation to new production varies significantly with time and space since N_2 fixation is more latitudinally variable than nitrate assimilation. Nitrate assimilation is fairly constant when the water column is well stratified; however, climatological events, including the ENSO event (Turk et al. 2001), and sporadic disturbances, such as wind-induced mixing (Eppley & Renger 1988) and mesoscale eddies (McGillicuddy et al. 1998), can increase the nitrate assimilation, thereby reducing the importance of the contribution of N_2 fixation for new production.

A certain degree of uncertainty may be associated with the estimation of new production due to possible nitrification. If the nitrification process strongly affects the presence of nitrates in the euphotic zone, as suggested in recent studies (Dore & Karl 1996, Yool et al. 2007, Raimbault & Garcia 2008), N_2 fixation can become the main source of new production in the western tropical and subtropical North Pacific Ocean and not just in the other areas with high N_2 fixation (Karl et al. 1997, Dore et al. 2002, Capone et al. 2005). The new production equals the export production in the steady state (Eppley & Peterson 1979), and it important to understand the efficiency of the biological pump amidst the growing concerns for global warming (Falkowski et al. 2000). N_2 fixation can become a key parameter for the evaluation of the sinking flux of particulate matter in the western tropical and subtropical North Pacific Ocean.

Acknowledgements. We thank S. Watanabe, K. Matsumoto, crew members and participants of the MR07-01 cruise for their cooperation at sea. We are grateful to H. Ogawa, K. Hayashizaki and M. C. Carvalho for their support in use of the mass spectrometer at Kitasato University. We greatly appreciate J. Kanda for insightful suggestions and T. Takemura for output of SPRINTARS. Thanks are also due to S. Kitajima for numerical abundance of microplanktonic diazotrophs. This research was financially supported by JSPS grants nos. 14658151, 17651003, 18067006 and 19030005.

LITERATURE CITED

Asaoka O, Marumo R (1987) An ecological study of marine planktonic blue-green algae, *Trichodesmium* (I)–Occurrence of *Trichodesmium* in various regions. Oceanogr Mag 57:1–14

Aufdenkampe AK, McCarthy JJ, Navarette C, Rodier M, Dunne J, Murray JW (2002) Biogeochemical controls on new production in the tropical Pacific. Deep-Sea Res II 49:2619–2648

Brown MT, Landing WM, Measures CI (2005) Dissolved and particulate Fe in the western and central North Pacific: results from the 2002 IOC cruise. Geochem Geophys Geosyst 6, Q10001. doi:10.1029/2004GC000893

Capone DG, Burns AJ, Montoya JP, Subramaniam A and others (2005) Nitrogen fixation by *Trichodesmium* spp.: an important source of new nitrogen to the tropical and subtropical North Atlantic Ocean. Global Biogeochem Cycles 19, doi:10.1029/2004GB002331

Deutsch C, Gruber N, Key RM, Sarmiento JL, Ganachaud A (2001) Denitrification and N_2 fixation in the Pacific Ocean. Global Biogeochem Cycles 15:483–506

Deutsch C, Sarmiento JL, Sigman DM, Gruber N, Dunne JP (2007) Spatial coupling of nitrogen inputs and losses in the ocean. Nature 445:163–167

Dore JE, Karl DM (1996) Nitrification in the euphotic zone as a source for nitrite, nitrate, and nitrous oxide at Station ALOHA. Limnol Oceanogr 41:1619–1628

Dore JE, Brum JR, Tupas LM, Karl DM (2002) Seasonal and interannual variability in sources of nitrogen supporting export in the oligotrophic subtropical North Pacific Ocean. Limnol Oceanogr 47:1595–1607

Dore JE, Letelier RM, Church MJ, Lukas R, Karl DM (2008) Summer phytoplankton blooms in the oligotrophic North Pacific Subtropical Gyre: historical perspective and recent observations. Prog Oceanogr 76:2–38

Dugdale RC, Goering JJ (1967) Uptake of new and regenerated forms of nitrogen in primary productivity. Limnol Oceanogr 12:196–206

Eppley RW, Peterson BJ (1979) Particulate organic matter flux and planktonic new production in the deep ocean. Nature 282:677–680

Eppley RW, Renger EH (1988) Nanomolar increase in surface layer nitrate concentration following a small wind event. Deep-Sea Res 35:1119–1125

Falkowski PG (1997) Evolution of the nitrogen cycle and its influence on the biological sequestration of CO_2 in the ocean. Nature 387:272–275

Falkowski P, Scholes RJ, Boyle E, Canadell J and others (2000) The global carbon cycle: a test of our knowledge of earth as a system. Science 290:291–296

Falkowski PG, Laws EA, Barber RT, Murray JW (2003) Phytoplankton and their role in primary, new, and export production. In: Fasham MJR (ed) Ocean biogeochemistry. Springer, New York, p 99–121

Favorite F, Dodimead AJ, Nasu K (1976) Oceanography of the subarctic Pacific Region, 1960–1971. Bull Int N Pac Fish Comm 33:1–187

Fernández C, Raimbault P, Garcia N, Rimmelin P, Caniaux G (2005) An estimation of annual new production and carbon fluxes in the northeast Atlantic Ocean during 2001. Geophys Res 110, C07S13, doi:10.1029/2004JC002616

Garcia N, Raimbault P, Sandroni V (2007) Seasonal nitrogen fixation and primary production in the Southwest Pacific: nanoplankton diazotrophy and transfer of nitrogen to picoplankton organisms. Mar Ecol Prog Ser 343:25–33

Grabowski MNW, Church MJ, Karl DM (2008) Nitrogen fixation rates and controls at Stn ALOHA. Aquat Microb Ecol 52:175–183

Hama T, Miyazaki T, Ogawa Y, Iwakuma T, Takahashi M, Otsuki A, Ichimura S (1983) Measurement of photosynthetic production of a marine phytoplankton population using a stable ^{13}C isotope. Mar Biol 73:31–36

Hansen HF, Koroleff F (1999) Methods of nutrient analysis. In: Grasshoff K, Kremling K, Ehrhardt M (eds) Methods of seawater analysis, 3rd edn. Wiley-VCH, Weinheim, p 159–228

Harrison WG, Harris LR, Irwin BD (1996) The kinetics of nitrogen utilization in the oceanic mixed layer: nitrate and ammonium interactions at nanomolar concentrations. Limnol Oceanogr 41:16–32

Hashihama F, Furuya K, Kitajima S, Takeda S, Takemura T, Kanda J (in press) Macro-scale exhaustion of surface phosphate by dinitrogen fixation in the western North Pacific. Geophys Res Lett, doi:10.1029/2008GL036866

Jickells TD, An ZS, Andersen KK, Baker AR and others (2005) Global iron connections between desert dust, ocean biogeochemistry, and climate. Science 308:67–71

Kanda J (2008) Vertical profiles of nitrate uptake obtained from *in situ* ^{15}N incubation experiments in the western North Pacific. J Mar Syst 71:63–78

Kanda J, Saino T, Hattori A (1985) Nitrogen uptake by natural populations of phytoplankton and primary production in the Pacific Ocean: regional variability of uptake capacity. Limnol Oceanogr 30:987–999

Kanda J, Itoh T, Ishikawa D, Watanabe Y (2003) Environmental control of nitrate uptake in the East China Sea. Deep-Sea Res II 50:403–422

Karl DM, Letelier RM, Tupas L, Dore JE, Christian J, Hebel DV (1997) The role of nitrogen fixation in biogeochemical cycling in the subtropical North Pacific Ocean. Nature 388:533–538

Kawakami H, Honda MC (2007) Time-series observation of POC fluxes estimated from ^{234}Th in the northwestern North Pacific. Deep-Sea Res I 54:1070–1090

Kustka A, Sañudo-Wilhelmy S, Carpenter EJ, Capone DG, Raven JA (2003) A revised estimate of the iron use efficiency of nitrogen fixation, with special reference to the marine cyanobacterium *Trichodesmium* spp. (Cyanophyta). J Phycol 39:12–25

Lee K, Karl DM, Wanninkhof R, Zhang JZ (2002) Global estimates of net carbon production in the nitrate-depleted tropical and subtropical oceans. Geophys Res Lett 29, doi:10.1029/2001GL014198

Levitus S (1982) Climatological atlas of the world ocean. NOAA Prof Pap 13, Washington, DC

Lipschultz F (2001) A time-series assessment of the nitrogen cycle at BATS. Deep-Sea Res II 48:1897–1924

McCarthy JJ, Carpenter EJ (1983) Nitrogen cycling in near-surface waters of the open ocean. In: Carpenter EJ, Capone DG (eds) Nitrogen in the marine environment. Academic Press, New York, p 487–512

McGillicuddy DJ Jr, Robinson AR, Siegel DA, Jannasch HW and others (1998) Influence of mesoscale eddies on new production in the Sargasso Sea. Nature 394:263–266

Millard RC, Owens WB, Fofonoff NP (1990) On the calculation of the Brunt-Väisälä frequency. Deep-Sea Res 37: 167–181

Montoya JP, Voss M, Kähler P, Capone DG (1996) A simple, high-precision, high-sensitivity tracer assay for N_2 fixation. Appl Environ Microbiol 62:986–993

Montoya JP, Holl CM, Zehr JP, Hansen A, Villareal TA, Douglas DG (2004) High rates of N_2 fixation by unicellular diazotrophs in the oligotrophic Pacific Ocean. Nature 430: 1027–1031

Moore JK, Doney SC, Lindsay K (2004) Upper ocean ecosystem dynamics and iron cycling in a global three-dimensional model. Global Biogeochem Cycles 18, doi:10.1029/2004GB002220

Needoba JA, Foster RA, Sakamoto C, Zehr JP, Johnson KS (2007) Nitrogen fixation by unicellular diazotrophic cyanobacteria in the temperate oligotrophic North Pacific Ocean. Limnol Oceanogr 52:1317–1327

Prakash S, Ramesh R, Sheshshayee MS, Dwivedi RM, Raman M (2008) Quantification of new production during a winter *Noctiluca scintillans* bloom in the Arabian Sea. Geophys Res Lett 35, doi:10.1029/2008GL033819

Raimbault P, Garcia N (2008) Evidence for efficient regenerated production and dinitrogen fixation in nitrogen-deficient waters of the South Pacific Ocean: impact on new and export production estimates. Biogeosciences 5:323–338

Suzuki R, Ishimaru T (1990) An improved method for the determination of phytoplankton chlorophyll using N,N-dimethylformamide. J Oceanogr Soc Jpn 46:190–194

Takemura T, Okamoto H, Maruyama Y, Numaguti A, Higurashi A, Nakajima T (2000) Global three-dimensional simulation of aerosol optical thickness distribution of various origins. J Geophys Res 105:17853–17873

Tomczak M, Godfrey JS (1994) Regional oceanography: an introduction. Pergamon Press, Oxford

Tsunogai S, Suzuki T, Kurata T, Uematsu M (1985) Seasonal and areal variation of continental aerosol in the surface air over the western North Pacific region. J Oceanogr Soc Jpn 41:427–434

Turk D, Lewis MR, Harrison GW, Kawano T, Asanuma I (2001) Geographical distribution of new production in the western/central equatorial Pacific during El Niño and non-El Niño conditions. J Geophys Res 106:4501–4515

Weiss RF (1970) The solubility of nitrogen, oxygen, and argon in water and seawater. Deep-Sea Res 17:721–735

Yan XH, Ho CR, Zheng Q, Klemas V (1992) Temperature and size variabilities of the Western Pacific Warm Pool. Science 258:1643–1645

Yool A, Martin AP, Fernández C, Clark DR (2007) The significance of nitrification for oceanic new production. Nature 447:999–1002

Editorial responsibility: Graham Savidge, Portaferry, UK

Submitted: July 14, 2008; Accepted: November 17, 2008
Proofs received from author(s): February 6, 2009